ELSEVIER

Highly polarized nuclear spin systems and dipolar interactions in NMR/Systèmes de spins nucléaires fortement polarisés et interactions dipolaires en RMN

Magnetic field dependence of proton spin-lattice relaxation of confined proteins

Jean-Pierre Korb [a,*], Robert G. Bryant [b]

[a] *Laboratoire de physique de la matière condensée, UMR 7643 du CNRS, École polytechnique, 91128 Palaiseau, France*
[b] *Chemistry Department, University of Virginia, Charlottesville, VA 22904-4319, USA*

Abstract

We present the magnetic field dependence of the proton spin-lattice relaxation rate $1/T_1$ in variously hydrated proteins and confined proteins in heavily hydrated gels where the protein molecular rotation has been immobilized. $1/T_1$ increases as a power law in the Larmor frequency at low magnetic field strengths. The linear temperature dependence of the protein proton $1/T_1$ demonstrates that relaxation results from a direct spin-phonon process instead of a Raman process above 273 K. We propose a theory that involves a simple characterization of the spatial distribution of the protons coupled with localized motions along and transverse to the polypeptide chain which accounts quantitatively for experiments. ***To cite this article: J.-P. Korb, R.G. Bryant, C. R. Physique 5 (2004).***

Résumé

Dépendance en champ magnétique de la relaxation spin-réseau du proton de protéines confinées. Nous présentons les dépendances en champ magnétique des vitesses de relaxation spin-réseau $1/T_1$ des protons de protéines plus ou moins hydratées ainsi que confinées dans des gels organiques réticulés pour bloquer la rotation. La relaxation $1/T_1$ augmente en loi de puissance à basse fréquence et varie linéairement avec la température. Ceci est cohérent avec un processus direct de relaxation spin-réseau plutôt que Raman au dessus de 273 K. Pour interpréter nos résultats nous proposons une théorie dépendant à la fois de la distribution des protons dans la structure et de la localisation des fluctuations parallèlement et transversalement aux chaînes peptidiques. ***Pour citer cet article : J.-P. Korb, R.G. Bryant, C. R. Physique 5 (2004).***

Keywords: Protein dynamics; Theory of spin-lattice relaxation; Confinement; Dipolar interaction; Localization; Fractal and spectral dimensions; Proton relaxation

Mots-clés : Dynamique de protéines ; Théorie de relaxation spin-réseau ; Confinement ; Interaction dipolaire ; Localisation ; Dimensions fractale et spectrale ; Relaxation dipolaire

1. Introduction

Proton spin-lattice relaxation rate measurements in chain molecules provide useful information for process control and characterization of materials. For instance, there is considerable current effort to understand how structural fluctuations in proteins and other macromolecules provide access to functional conformations or provide energetic couplings that result in

---

* Corresponding author.
  E-mail address: jean-pierre.korb@polytechnique.fr (J.-P. Korb).

concerted and crucial changes in location or concentration as in muscle contraction or active transport [1–3]. The dynamical spectrum of a folded polymeric structure is complex and characterization requires examination over many decades in frequency or time. High resolution NMR is usually restricted to dynamical characterization in the time range of ns or shorter; however, the nuclear magnetic spin-lattice relaxation dispersion (NMRD) provides a powerful approach to this class of problems because variations of the experiment may probe intra and intermolecular dynamics from the range of milliseconds to picoseconds [4].

We report proton magnetic relaxation dispersion measurements of $1/T_1$ on lyophilized proteins (lysozyme and BSA) at various temperatures. The magnetic field dependence of proton proteins $1/T_1$ in such dry proteins may be represented by a power law: $1/T_1 = A\omega^{-b}$ where b is usually found to be 0.78. We also observe a linear temperature dependence of $1/T_1$ in a large range of low frequencies. These data confirm our model previously published [5,6] and outlined in the first part of the theoretical section. According to this model, the power law may derive from localized structural fluctuations along the backbone of the peptide chain that modulate the proton–dipole–dipole couplings. The theory provides a quantitative evaluation of both A and b from first principles based on a direct spin-phonon process that is made dramatically more efficient because of the restricted propagation in the chain molecule. The relaxation dispersion profile characterizes the low frequency distribution of vibrational states in the folded protein system.

We also report proton magnetic relaxation dispersion measurements (NMRD) of $1/T_1$ on proteins progressively hydrated and rotationally immobilized proteins confined in cross-linked organic gels. The experiments have been repeated at various temperatures and pH values. The spectroscopic price of immobilization is loss of the high resolution spectra usually associated with proton NMR spectroscopy; however, the magnetic relaxation dispersion measurements provide a valuable characterization of the intramolecular protein dynamics at frequencies well below the rotational frequency of the protein in solution. This method allows studying such a dynamics in native condition and in a very large range of time scales. Although, the situation is more complex in dynamically and molecularly heterogeneous systems such as biological tissues, the functional dependencies observed in the protein cases are basically reproduced in the more complex cases [7–9]. In the high frequency range of our experiments on more or less hydrated proteins, the magnetic field dependences of protons are still represented by a power law $1/T_1 = B\omega^{-b}$, where an expression for B is found and b is usually decreasing from 0.8 to 0.6, when increasing the degree of hydration. However, a cross over to a frequency independent value appears at low frequency. The value of such plateau decreases with hydration.

These experimental data confirm a previously published theory [5,6] outlined in the second part of the theoretical section. Basically this theory couples the liquid and solid spin population responses and accounts quantitatively for the observed magnetic field dependence of proton spin-lattice relaxation in immobilized and hydrated protein systems. Two parameters are extracted from a comparison with the experimental data: (i) the fractal dimensionality d_f of the spatial proton distribution in the macromolecular matrix that is found to decrease continuously with hydration; (ii) the spin exchange rate constants between the macromolecule protons and the water protons, which is simply related to the number of long-lived water molecule sites as well as to the number of labile protons and their exchange lifetimes. This shows that the protein structure adjusts to hydration from the lyophilized state to the fully hydrated state in small increment steps.

This two-parameter model is easily generalized to more complex systems, such as tissues, because all rotationally immobilized molecules that contribute are linear polymers with relatively few cross-links. It is also central to a fundamental understanding of the factors that control signal intensity and information content in magnetic resonance images (MRI).

2. Experiments

The ^{1}H NMR spectrum of a rotationally immobilized protein, whether it is in a lyophilized powder or a heavily hydrated gel is broad and all sharp features are lost in the linewidth, which is typically approximately 25–30 kHz [10]. However, it is well known that when proteins are hydrated, even though the systems remains solid and the proteins do not rotate, the proton spin-lattice relaxation rate of the water and the protein protons are coupled. In fact, the magnetic field dependence of the solid is mapped onto the solvent protons. The protein protons are strongly coupled by dipole–dipole interactions between protons and the linewidth is homogeneous; irradiation in any portion of the line saturates the whole line, which is an important basis for magnetic transfer contrast imaging in diagnostic medicine. The protein protons in a folded protein structure form a three-dimensional network where the connections derive from the strong dipolar coupling. Spin communication or spin diffusion is efficient and generally there is no gradient of spin temperature within the protein proton spin system at room temperature [11]. Stated differently, the strong connectivity of the proton spin system provides a globally sensitive system that may be used to interrogate the dynamics of the molecule.

The magnetic field dependence of the proton spin-lattice relaxation rate, $1/T_1$, or the nuclear magnetic relaxation dispersion, *NMRD*, provides a direct characterization of the noise spectrum that causes modulation of the magnetic energies of the protons. Fig. 1 shows typical proton relaxation dispersion data for two lyophilized proteins, bovine serum albumin (*BSA*) and lysozyme, obtained using a fast field cycling spectrometer from *Stelar Instruments, Mede, Italy*. The lyophilization procedure is described
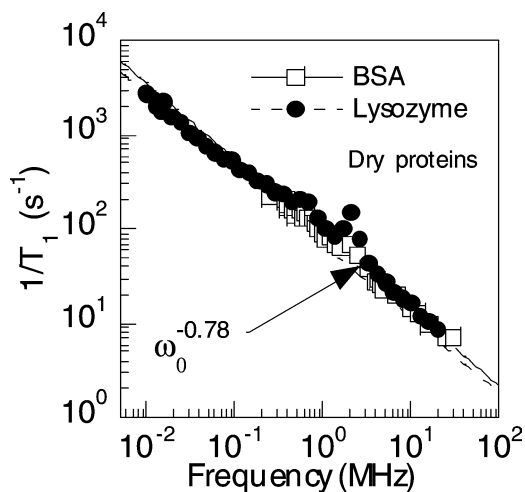
Fig. 1. The proton spin-lattice relaxation rate recorded as a function of the magnetic field strength plotted as the proton Larmor frequency for samples of dry lysozyme and BSA. The solid line presents the best fit of the data with Eqs. (3), (4) and $b = 0.78$. This value of b leads to a value $d_f = 3$ from Eq. (4), which indicates a uniform distribution of protons. The peaks at 2.8, 2.4 and 0.8 MHz in the relaxation rate profile are caused by proton relaxation coupling to the amide nitrogen when the ^{14}N energies match the proton Zeeman levels.
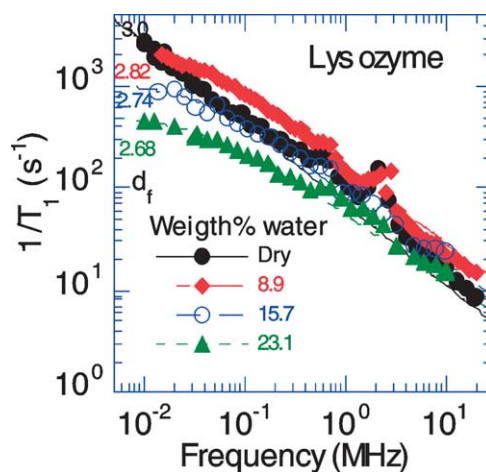

Fig. 2. The proton spin-lattice relaxation rate recorded as a function of the magnetic field strength plotted as the proton Larmor frequency for lysozyme samples hydrated to various degrees (%). The solid lines are the best fits to the data using Eq. (5) with R_P given by Eqs. (7b) and (4). The two parameters adjusted are R_{WP} and b. The value d_f is obtained from b according to Eq. (4).
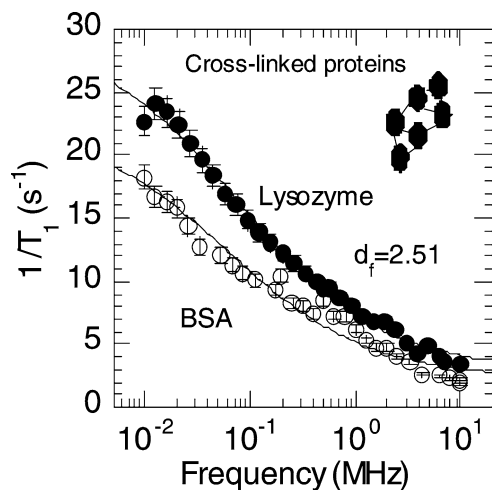

Fig. 3. The proton spin-lattice relaxation rate recorded as a function of the magnetic field strength plotted as the proton Larmor frequency for samples of cross-linked lysozyme and *BSA*. The solid lines are fits to the data using Eq. (5) with R_P given by Eqs. (7(b)) and (4). The two parameters adjusted are R_{WP} and $b = 0.6$ giving $d_f = 2.51$.
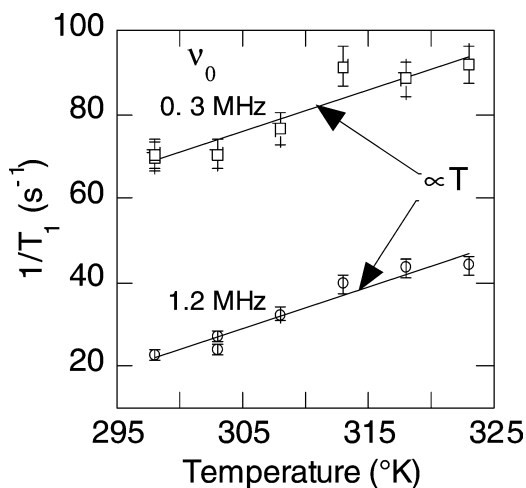

Fig. 4. Temperature dependence of the proton spin-lattice relaxation rates of hydrated lysozyme at two different frequencies.

in [7]. For the protons in both systems, the relaxation rate is a power law with the Larmor frequency: $1/T_1 \propto A\omega_0^{-b}$ with $b = 0.78$. Fig. 2 shows the magnetic field dependence of the proton spin-lattice relaxation rate $1/T_1$ in variously hydrated proteins. A plateau appears in the field dependence at low field strengths, the absolute value of which decreases with increasing levels of hydration. We present also the case of lysozyme confined in heavily hydrated gels where the rotation has been

immobilized by cross-linking with glutaraldehyde (Fig. 3). The data for cross-linked BSA are similar (Fig. 3). The linear temperature dependence of the protein proton spin lattice relaxation rate constant $1/T_1$ shown in Fig. 4 demonstrates that proton-spin relaxation results from a direct spin-phonon process rather than a Raman process at temperatures above 273 K that is proportional to the square of temperature [12]. The absence of significant pH dependence in the proton relaxation rates obtained in serum albumin gels implies that the effective magnetization transfer rate between water and the protein is not dominated by proton transfer processes, which would be strongly pH dependent.

3. Theory

3.1. Proton spin lattice relaxation rate R_p in a direct process for a dry protein

Crudely, the power law observed in Fig. 1, with $b = 0.78$, provides an indication of the power spectrum of the fluctuations, i.e., the noise, present in the protein. Kimmich and coworkers found a similar b value for other proteins and polypeptide systems [13]. They show that such an exponent, b, is not a function of the side chain, and suggested that the backbone dynamics drive the relaxation process [13]. However, they did not offer a detailed theory for the protein systems studied. We have addressed this question in detail based on a quantitative model that accounts for the power law dependence [5,6].

Here, we just outlined the essence of the proposed theoretical development for the protein-proton relaxation rate R_p. First, due to the temperature dependence shown in Fig. 4, the theory is built on an extension of models of relaxation caused by a direct spin-phonon interactions, not indirect or Raman process [12]. Two factors make the spin-phonon coupling efficient in the low frequency range probed here: (i) the motions that drive relaxation are associated with the backbone of the polypeptide chain so that the propagation of the disturbance is not in three dimensions, but largely restricted to one. In consequence, the vibrational density of states is dramatically enhanced in the low frequency range compared with usual 3D cases [14]: (ii) the disturbance is localized and the spatial extent is related to the frequency of the fluctuation. The spin displacement is expanded on a localized basis of planar waves of different wavelengths, the propagation of which is spatially bounded. In fact, scaling arguments show that the product of the volume of localization, V_α, for a given frequency ω_α and the number of modes, N_α, outside this volume, V_α, is a constant [15] which results in anomalous dispersion relations:

$$V_\alpha N_\alpha = \ell_\alpha^{d_f} \int_0^{\omega_\alpha} \sigma(\omega)\,d\omega = \ell_\alpha^{d_f} \omega_\alpha^{d_s} = Cte, \tag{1}$$

where $\sigma(\omega) \propto \omega^{d_s-1}$ is the density of vibrational states, $d_s \sim 4/3$ is the spectral dimension that characterizes the anomalous propagation of the disturbance [16,17], ℓ_α is the radius of localization associated with the planar waves of frequency ω_α. It follows from Eq. (1) that the radii of localization at the two extremes of our frequency range ($\omega_{\min} = 2\pi \times 10^{-2}$ MHz, $\omega_{\max} = 2\pi \times 10^2$ MHz) follow the scaling relation:

$$\frac{\ell_{\max}}{\ell_{\min}} = \left(\frac{\omega_{\max}}{\omega_{\min}}\right)^{d_s/d_f} \approx 50. \tag{2}$$

In consequence, the effective size of the space explored changes from essentially the limit of the bond lengths $\ell_{\min}$ to distances of the order of the approximate size of the protein molecule $\ell_{\max}$; i.e., from of order 1 to of order 50 Å.

The theory presumes that localized displacements modulate the proton dipolar couplings, and the effects are then transmitted to the whole proton network by rapid spin diffusion. The proton distribution in space is characterized by a fractal dimension, d_f, which may be also computed from the x-ray crystal structure [14,18] and characterizes the proton-proton magnetic connectivity which is different from the connectivity that propagates the disturbance that drives relaxation (d_s) [16,17]. A theoretical development presented recently [5], considered explicitly the time fluctuations induced by localized longitudinal motions of the protein backbone. This model gives for the proton spin-lattice relaxation rate R_p induced by a direct spin-phonon process the following analytical expression of the form $R_p = A\omega^{-b}$, where A and b are given by:

$$R_p^{\text{longitudinal}} = \frac{27\pi\beta}{20} d_s \left(\frac{k_B T}{\hbar}\right) \left\{ \left(1 + \frac{1}{2^b}\right) \left(\frac{\hbar\omega_{\text{dip}}}{\Delta E_{v\parallel}}\right)^2 \left(\frac{\hbar\omega_0}{\Delta E_{v\parallel}}\right)^{-b} \right\} \tag{3}$$

with

$$b = 3 - \frac{2d_s}{d_f} - d_s. \tag{4}$$

Here, d_f is the fractal dimensionality of the proton distribution in space, β is a numerical factor ($\beta > 1$) associated with the effective size of the proton dipolar coupling ω_{dip} [5]. $\Delta E_{v\parallel}$ is the energy of the highest vibrational modes relevant of the system
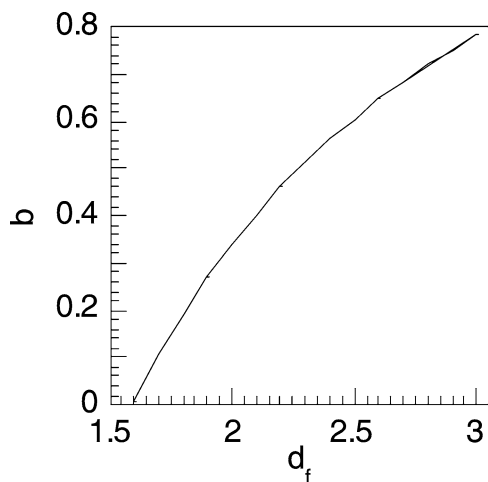
Fig. 5. Variation of the exponent *b*, given by Eq. (4), with the fractal dimension df characterizing the distribution of protein protons and $d_s = 4/3$.
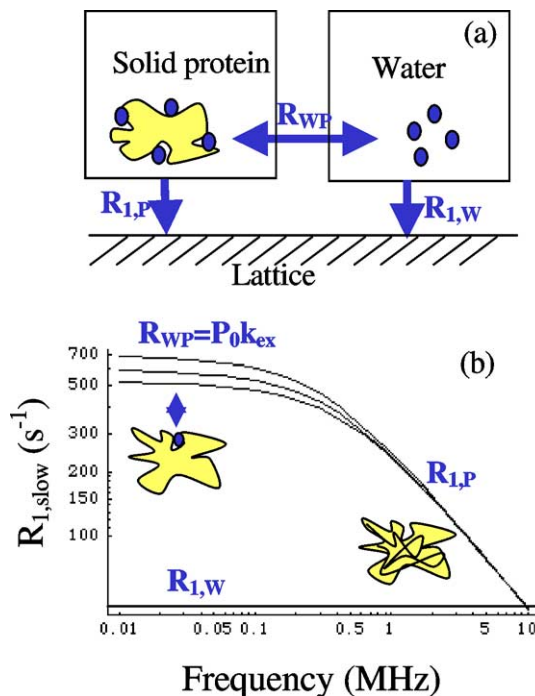

Fig. 6. (a) Schematic diagram showing that the spin-lattice relaxation of water protons is dynamically coupled to the solid protein protons. (b) Typical theoretical frequency dependence of the proton spin-lattice relaxation rate R_{slow} for hydrated protein. The schematic diagrams given in insert summarize the dynamical information obtained in the high and low frequency ranges.

parallel to the direction of the backbone, and taken as the amide (II) mode at 1560 cm^{-1} [18]. This vibrational energy enters the calculation as the high frequency limit of the density of vibrational states associated with the protein system. Although there are usually 3*N* modes in a solid of *N* atoms, this estimate does not include the very soft contributions associated with inter chain potentials, side–chain–side chain interactions, which partly have the character of intermolecular motions except that they are between different components of the same long chain.

We have displayed in Fig. 5 the variation of the exponent *b* of this power law with the fractal dimension d_f characterizing the distribution of protein protons. According to Eq. (4), *b* varies continuously from 0 for $d_f = 5/3$ to a maximal value of 0.78 for $d_f = 3$. It is worthwhile to note that for $b = 0$, the value of $d_f = 5/3$ that results corresponds to the dimension of self avoiding chains. According to this theory, the limiting value $b = 0.78$ is clearly associated to a uniform distribution of protons when d_f approaches the Euclidean value of 3. This result observed for lyophilized proteins and various polypeptide systems thus makes sense in that the protein or peptide system is not native or is denatured to some extent by the dehydration process. Hydration causes structural changes in the protein as it approaches a native folded structure that changes the uniformity of the proton distribution in space, and thus d_f.

3.2. Proton spin lattice relaxation rate in a direct process for a hydrated protein

In this model, the spin-lattice relaxation of water protons is dynamically coupled to the solid protein protons (Fig. 6(a)). In most applications of both imaging and field cycling experiments, the rapidly decaying component of the bi-exponential decay is not detected because of instrumental limitations and the slowly decaying component R_{slow} dominates the observations. This rate constant component R_{slow} is a function of the relaxation rate constants that characterize the coupling of each population to the lattice as well as the rate constant for the inter-population communication as given by:

$$R_{slow} = \frac{1}{2}\left\{ R_w + R_p + R_{wp}\left(1 + \frac{1}{F}\right) - \left[\left(R_p - R_w - R_{wp}\left(1 - \frac{1}{F}\right)\right)^2 + \frac{4R_{wp}^2}{F}\right]^{1/2}\right\}, \tag{5}$$

where R_w and R_p are the spin-lattice relaxation rate constants for the water and protein protons, respectively [7]. F is the ratio of the protein-proton to water-proton populations at equilibrium [6,7]. R_w ($\approx s^{-1}$) is assumed to be independent of the Larmor frequency within the frequency range studied here because the bulk water motion is very rapid, even at the surface of the protein. R_{wp} is the cross-relaxation rate constant between the proton-water and the protein-protons. A theoretical development presented recently [5], considered explicitly the time fluctuations induced by localized longitudinal and librational motions of the protein backbone. This model gives for R_p two contributions $R_{p,\text{longitudinal}}$ and $R_{p,\text{librational}}$ coming from these two motions:

$$R_p = R_{p,\text{longitudinal}} + R_{p,\text{librational}},\tag{6}$$

where

$$R_p^{\text{longitudinal}} = \frac{27\pi\beta}{20}d_s\left(\frac{k_B T}{\hbar}\right)\left\{\left(1+\frac{1}{2^b}\right)\left(\frac{\hbar\omega_{\text{dip}}}{\Delta E_{v\parallel}}\right)^2\left(\frac{\hbar\omega_0}{\Delta E_{v\parallel}}\right)^{-b}\right\},\tag{7a}$$

$$R_p^{\text{librational}} = \frac{3\pi\beta}{10}d_s\left(\frac{k_B T}{\hbar}\right)\left\{\left(\frac{7}{2}+\frac{1}{2^b}\right)\left(\frac{\hbar\omega_{\text{dip}}}{\Delta E_{v\perp}}\right)^2\left(\frac{\hbar\omega_0}{\Delta E_{v\perp}}\right)^{-b}\right\}\tag{7b}$$

and b is given in Eq. (4). We show in Fig. 6(b) a typical theoretical frequency dependence of R_{slow} for hydrated protein. We clearly see in Fig. 6(b) two different relaxation behaviors: the power law dependence in the high frequency range and the plateau at low field. We saw above that the power law is due to slow fluctuations propagating along or transverse to the backbone. We show below that the value of the limiting value of the relaxation rate observed in the plateau region is associated with the exchange rate of long-lived water molecule with the water pool.

3.3. Cross-relaxation and water spin couplings in proteins

In Eq. (5), R_{wp} is the cross-relaxation rate constant between the proton-water and the protein-protons. We find no significant pH dependence of this effective magnetization transfer rate in the serum albumin gels. This experimental fact and the following arguments have allowed us to propose a theoretical expression for R_{wp}.

In protein solutions, there are two exchange mechanisms that couple the dynamical properties of the protein to the solvent proton relaxation: exchange of whole water molecules, and exchange of water protons with functional groups of proteins such as RNH_3^+. At near neutral pH and higher pH, Halle among others has shown that the proton exchange contribution may be as large or larger than the whole water molecule exchange contribution for proteins in solution [19,20]. However, we find no pH dependence of the effective magnetization transfer rate in the serum albumin gels studied even though the kinetic equations above should describe the proton exchange contributions accurately. Therefore, we must conclude that when the protein is a solid, i.e., when the rotational motion is stopped or very slow compared with the proton–proton dipole–dipole coupling, the proton exchange pathway for solvent spin coupling to the protein spin relaxation is unimportant. That is, although both water exchange and proton exchange contributions are present, when the rotational motion of the protein is stopped, the whole water molecule pathway becomes completely dominant.

This observation is reasonably explained by the following chemical and physical argument. The exchange rates for whole water molecules with protein sites are independent of whether the protein is freely rotating or not. This is also true for the protons exchanging with labile groups like amines or RNH_3^+. In each case, we may write that the relaxation rate of the observed water proton signal is given at low frequency by:

$$\frac{1}{T_1} = \sum_{i,\text{sites}}^{N}\frac{P_i}{T_{1,\text{solid}}+\tau_{\text{ex},i}},\tag{8}$$

where the sum runs over water molecule sites and over proton sites on the protein, P_i is the probability that a proton occupies the ith site on the protein, $\tau_{\text{ex},i}$ is the effective exchange time. Previous work has shown that R_{WP} does not depend on the strength of the magnetic field because the magnetization transfer rate is limited by the spin–spin relaxation time $T_2 = 12\,\mu s$ of the solid phase [6,9]. Then we may write,

$$R_{WP} = P_0\sum_{i,\text{sites}}^{N}\frac{1}{T_{2,\text{solid}}+\tau_{\text{ex},i}} = P_0 k_{\text{ex}},\tag{9}$$

where k_{ex} is the sum over the effective exchange contributions from each site and $P_0 = nF/N_H$ is the probability for a labile protein site exchanging with water. Here n is the number of exchanging protons at the site and N_H is the number of protons in the protein (973 for lysozyme). The effective exchange times τ_{ex} must be on the order of 1 µs or faster for whole water molecules. If it were not the case, we would see the low field plateau occurring at a much lower relaxation rate than it does.

Thus, it is now a sound conclusion that although there is a distribution of water molecule lifetimes, the distribution spans about a decade between 10^{-6} and 10^{-7} s for the $n = 25$ bound water molecules in BSA. Therefore, for whole water molecule exchange, the $\tau_{\mathrm{ex},i}$ in Eq. (9) is 1 μs or shorter. $T_{1,\mathrm{solid}}$ is the protein proton T_1 which is generally not nearly that short. Thus, the exchange rate makes almost no contribution to the relaxation equation for the labile water molecules when the protein is immobilized except possibly at the very lowest field.

On the other hand, the proton exchange rates with protein functional groups are relatively slow. For ammonia, the high resolution lines are just broadening some at pH $= 3$–4, so the exchange rates are in the range of 100 s^{-1} or slower, depending of course of temperature. So the labile proton exchange rates have to change considerably before the exchange rate becomes negligible in the denominator of Eq. (9). Furthermore, the labile proton sites like RNH_3^+ usually stick out in the solution and these protons are not always very well coupled magnetically with the rest of the protein because local motions of the tethered site reduce the effective dipolar coupling to the rest of the protein. Thus, the cross-relaxation is not as efficient compared with the more buried water molecule sites. For a buried water molecule site, the protein-proton water-proton cross relaxation rate is approximately the $1/T_2$ for the protein proton spins when rotationally immobilized, or $1/12$ μs. In solution, the cross-relaxation rate is not nearly as large because of rotational averaging of the dipole-dipole couplings.

The problem is less clear in the case of a lyophilized powder or a slightly hydrated powder because one cannot easily define the pH. There is no bulk solution in this case and proton concentration is an elusive concept in the absence of a completely continuous solution phase. One can define the pH of the solution from which the protein powder was prepared by lyophilization, which defines the ionization state of the protein. What we find is that the ionization state (pH of the preparation solution) does not change the observed MRD profile significantly, therefore the ionization state of the protein over the preparation range of pH values of 4–8 is unimportant as a determinant of the cross-relaxation rate.

In summary, for both the gel, where the argument is on firm ground, and in the powders, there is no significant pH dependence. There would be a strong pH dependence if proton exchange were an important mechanism for magnetization transfer from the protein to the solvent spins. Thus, the water must carry the magnetization transfer via whole molecule exchange pathways.

4. Comparison experiments versus theory

The solid line through the data obtained for two lyophilized proteins (lysozyme and bovine serum albumin) displayed in Fig. 1 is obtained using nonlinear least squares fit of Eqs. (3) and (4) where only the parameter b was permitted to vary. The other parameters used are: $d_s = 4/3$, $\omega_{\mathrm{dip}}/2\pi = 11$ kHz, with $\beta = 3$ as discussed previously [5]. One finds $b = 0.78$ for the two lyophilized proteins and b decreasing from 0.78 to 0.6 when increasing the degree of hydration using Eqs. (4), (5), (7(b)).

For the proteins studied here, we find from the X-ray data [14,21] $d_f = 2.52$ for the fully hydrated crystal environment which implies that the 3-dimensional structure of the protein does not provide a perfectly uniform density of protons. We have previously noted, that when the protein is lyophilized, the experimental NMRD characterization of d_f, approaches the value of 3 (through the value of b in Eq. (4) (Fig. 5), which implies that in the lyophilized state, the protein distribution is more uniform as the tertiary structure is collapsed by the removal of solvent. Thus, owing to Eq. (4) and Fig. 5 the value of b in the lyophilized cases above approaches the limiting value of 0.78 and d_f approaches the Euclidean value of 3. Such a result appears to be generalized also to amino-acid polymers [13] justifying the quasi one-dimensional dynamics along the primary structure.

The good agreement with the theory (continuous lines in Figs. 1–3), where an excellent fit to the data is obtained with only one adjustable parameter, b, indicates that the ^{1}H relaxation dispersion experiment provides important view of the protein dynamics. The data require that the density of modes in the protein is not strongly attenuated by lowering the frequency as usual in 3-dimensional system, but is held up drastically by the quasi-one-dimensional character of the polypeptide chain system. This results in a density of vibrational modes characterized by a very weak frequency dependence proportional to $\sigma(\omega) \sim \omega^{d_s-1} = \omega^{0.33}$. Further, the interconnectivity of the proton network monitors the dynamics of the whole protein system simultaneously; however, the character of the relaxation events required by the theory are localized structural fluctuations. We have shown that such a localization gives a supplementary frequency dependence as ω^{2d_s/d_f} [5]. The picture is closely related to the concept of mobile defects in proteins [22]. The increase in relaxation efficiency at low frequency results in part because the longer wavelength disturbances permitted by the lower frequency directly modulate more proton-proton couplings. It is important to note that although we have used the language of vibrational motions, the dispersion shown in the experiment demonstrates that the motion is stochastic rather than periodic.

As shown also in Figs. 2 and 3 and 6(b), the addition of water changes the relaxation profile significantly at low frequency. Several features are critical: The spin relaxation of the protein protons are coupled to the water protons, which causes the relaxation rate to be reduced in proportion to the ratio of protein spins to the water spins. The basic field dependence is preserved. The protein structure rearranges in the presence of water to achieve the native fold, which may change the distribution of protons in space and is reflected in the parameter, d_f. The longitudinal fluctuation modes along the peptide chain of the protein are not
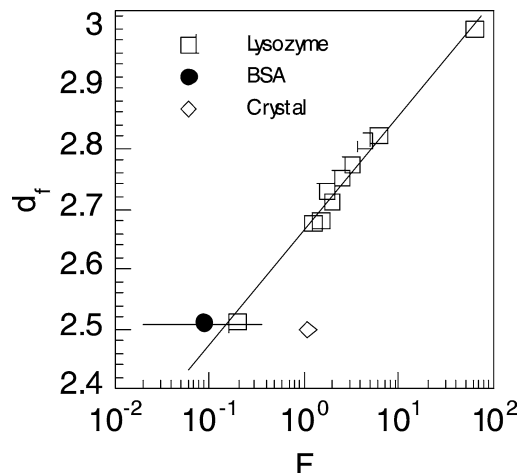
Fig. 7. The fractal dimension df of the proton distribution obtained from Fig. 2 and recorded as the ratio F between the protein-protons and the water-protons at equilibrium. The continuous line is a logarithmic fit of the data.

sufficient to account for the relaxation. The addition of water permits transverse low frequency modes to operate, which adds a second term to the relaxation equation (see Eq. (7b)) that is found to dominate the relaxation for hydrated proteins.

The absence of pH dependence observed in the relaxation dispersion demonstrates that R_{wp} is dominated by chemical exchange of long lived water molecules (~ 1 μs) embedded in the protein with the bulk water pool.

As shown in Fig. 2, the hydration reduces the value of b from 0.78 to 0.6, which reflects reduction of d_f from 3 to 2.5 which is consistent with the fractal dimension of the proton distribution deduced from the X-ray crystal structures. We show in Fig. 7, the variation that we observe for d_f with the parameter F which is the ratio of the protein-proton to water-proton populations at equilibrium. The logarithmic dependence observed shows that the protein structure adjusts to hydration from the lyophilized state ($F \sim 10^2$) to the fully hydrated state ($F \sim 10^{-1}$) in small increment steps. The fact that after completion of all the hydration sites of two different proteins, the value of d_f reaches the constant value of 2.5 makes sense and proves the universality of the proposed method.

5. Conclusion

We have presented proton relaxation dispersion experiments of more or less hydrated proteins and proteins confined in gel by cross-linking. The data have been interpreted through a theory that accounts for experiments and depends on the dynamical distribution of vibrational states, the localization of the disturbances along and transverse to the peptide chains, and the spatial distribution of protons in the protein structure. The spatial distribution of protons in the protein is characterized by a fractal dimension d_f that is found to decrease continuously with hydration. This gradual change with hydration shows that the protein structure adjusts to hydration from the lyophilized state to the fully hydrated state in small increment steps.

References

 [1] B.F. Rassmussen, A.M. Stock, D. Ringe, G.A. Petsko, Nature 357 (1992) 423.
 [2] L. Vitagliano, A. Merlino, A. Zagari, L. Mazzarella, Proteins 46 (2002) 97.
 [3] E. Perozo, A. Kloda, D.M. Cortes, B. Martinac, Nature Struct. Biol. 9 (2002) 696.
 [4] A. Noack, NMR Spectrosc. 18 (1986) 171.
 [5] J.-P. Korb, R.G. Bryant, J. Chem. Phys. 115 (2001) 10964.
 [6] J.-P. Korb, R.G. Bryant, Magn. Reson. Med. 48 (2002) 21.
 [7] C.C. Lester, R.G. Bryant, Magn. Reson. Med. 21 (1991) 117.
 [8] C.C. Lester, R.G. Bryant, Magn. Reson. Med. 22 (1991) 143.
 [9] R.G. Bryant, Annu. Rev. Biophys. Biomol. Struct. 25 (1996) 29–53.
[10] W.M. Shirley, R.G. Bryant, J. Amer. Chem. Soc. 104 (1982) 2910.
[11] H.T. Edzes, E.T. Samulski, J. Magn. Reson. 31 (1978) 207.
[12] A. Abragam, The Principles of Nuclear Magnetism, Clarendon Press, Oxford, 1961.

[13] R. Kimmich, F. Winter, Progr. Colloid Polym. Sci. 71 (1985) 66.
[14] J.-P. Korb, A. Van-Quynh, R.G. Bryant, Chem. Phys. Lett. (2001) 339.
[15] S. Alexander, Phys. Rev. B 40 (1989) 7953.
[16] S. Alexander, R. Orbach, J. Phys. Lett. (France) 43 (1982) L625.
[17] E. Courtens, R. Vacher, J. Pelous, Th. Voignier, Europhys. Lett. 6 (1988) 245.
[18] T. Miyazawa, T. Shimanouchi, S. Mizushima, J. Chem. Phys. 29 (1958) 611.
[19] B. Halle, V.P. Denisov, Biophys. J. 69 (1995) 242.
[20] B. Halle, V.P. Denisov, K. Venu, in: Biological Magnetic Resonance, vol. 17, Kluwer Academic/Plenum, New York, 1999, p. 419.
[21] B.W. Matthews, J. Mol. Biol. 33 (1968) 491.
[22] R. Lumry, A. Rosenberg, L'eau et Les Systèmes Biologiques 246 (1976) 53.